

03,12

Modeling structural and energy characteristics of atoms in a GaS 2D-crystal with point defects

© M.M. Asadov^{1,2}, S.N. Mustafayeva³, S.S. Guseinova³, V.F. Lukichev⁴, D.B. Tagiev¹

¹ Nagiyev Institute of Catalysis and Inorganic Chemistry named after Academician M. Nagiyev, Azerbaijan National Academy of Sciences,

Baku, Azerbaijan

² Scientific Research Institute of Geotechnological Problems of Oil, Gas, and Chemistry,

Baku, Azerbaijan

³ Institute of Physics, Azerbaijan National Academy of Sciences,

Baku, Azerbaijan

⁴ Valiev Institute of Physics and Technology, Russian Academy of Sciences,

Moscow, Russia

E-mail: mirasadov@gmail.com

Received July 31, 2021

Revised September 5, 2021

Accepted September 6, 2021

The properties of hexagonal gallium monosulphide (GaS) were modeled within the framework of the density functionality theory (DFT) taking into account the impact of vacancies related to a short range ordered structure. It is shown that electron irradiation of a GaS monolayer causes a decrease in conductivity due to formation of point defects. The band structure, density of states and energy properties of GaS supercells with 36 and 48 atoms with monovacancies were calculated. DFT calculations were performed to obtain values of the formation energy of GaS and Ga and S atom vacancies, as well as to determine the degree of vacancies' impact on the properties. Impact of GaS compound composition on the chemical potential value was studied taking into account the Ga-S phase diagram.

Key words: modeling, DFT calculation, GaS supercells, point defects, energy structure, density of states, formation energy, chemical potential.

DOI: 10.21883/PSS.2022.01.52487.182

1. Introduction

Interest to two-dimensional (2D) layered materials based on semiconductor compounds of type $A^{III}B^{VI}$, for which quantum effects are typical, is conditioned by the potential of their application in nanodevices [1,2]. Covalent bond acts in 2D-crystals of $A^{III}B^{VI}$ in layers due to overlapping of valence orbitals, while weak Van der Waals bond (several kJ/mol) acts between the layers [3]. Such a bond between the layers can form, in particular, due to the dispersion effect (interaction of instantaneous dipoles arising in atoms (or molecules) due to a temporary shift of electron orbits and nuclei). The layered semiconductor gallium monosulphide (GaS) is a material with an indirect band gap ΔE_g equal to ~ 2.53 eV at 77 K [3]. GaS can be applied in optoelectronic devices in the visible range and has been studied for rather a long time. The results of physical/chemical [3] and physical [4] studies of GaS have been systematized in reference books. Information about impurities' impact on properties of GaS for manufacture of high-quality devices, in particular, is given in the paper [5]. A modification of the GaS compound has a hexagonal layered structure of GaS type [3,4,6,7].

GaS has a number of advantages over other 2D-materials: a wide region of operating temperatures, the possibility

to create light-emitting devices in a broad spectrum on their basis, high values of electric breakdown critical field, radiation resistance. A layered GaS crystal has both the Ga-S and Ga-Ga bonds. Each layer consists of S-Ga-Ga-S packs, where each gallium atom is tetrahedrally surrounded by three sulfur atoms and one gallium atom. S-Ga-Ga-S packs may have different stacking, which explains the existence of gallium monosulphide polytypes. GaS has high photoelectric, optoelectronic and anisotropic properties. Depending on layer stacking in the GaS crystalline structure, four GaS polytypes are distinguished (β , ϵ , γ and δ). The hexagonal phase of GaS (spatial group (sp.gr.) $P6_3/mmc$) [1,7], i.e. the β -polytype of GaS is an energetically favorable crystalline arrangement. The thermodynamically stable modification at room temperature is β -GaS. One β -GaS layer consists of repeating units S-Ga-Ga-S formed by six-membered Ga_3S_3 rings. Thereat, the adjacent GaS layers are held together along the crystal c -axis by Van der Waals forces.

Distribution of electron density in a hexagonal elementary cell of GaS (spatial group (sp.gr.) $P6_3/mmc$), $a = 3.592(1)$ Å, $c = 15.465(3)$ Å) has been studied experimentally and by the pseudopotential method taking into account the bond between the nearest neighbors Ga-Ga (2.449 Å) and Ga-S in the crystal [7]. It was shown that,

according to experimental data, chemical bonds exist in GaS not only between the nearest neighboring atoms Ga-S and Ga-Ga in an elementary cell, but there are also bonds between Ga and S with the next nearest neighbors in the same elementary cell and with atoms in the surrounding elementary cells. The pseudopotential method cannot predict the type of the said chemical bonds in GaS [8,9]. This is related to an unusual electron density in GaS, where atoms are not densely packed and components' valencies (groups III and VI) do not coincide.

Studies of the properties, structure and possibilities of application of nanosized 2D-semiconductors of GaS type by density functionality theory (DFT) methods are being continued. The phonon spectrum of the β -GaS crystal was calculated in the paper [8] in a local density approximation (LDA). Elastic constants and sound velocities along and across the layers were determined. The paper [9] presented *ab initio* calculations of the dependence of the folding energy and band gap for GaS nanotubes on their diameter. It was shown that dependence of the folding energy on diameter meets the inverse-square law and is identical for nanotubes of the „zigzag“ and „armchair“ types.

Anisotropic properties also manifest themselves in GaS-based nanomaterials. Compounds with a structure of GaS type have optical and electric properties [10–13] close to 2D-materials of the nanotechnology, e.g., graphene [14] and topological insulators [15].

As distinct from other metal monochalcogenides, e.g., GaSe [9,10], GaS bulk crystals at room temperature have a wider optical band gap (ΔE_g) (at 300 K: indirect $\Delta E_g \sim 2.5\text{--}2.6\text{ eV}$ [16], and direct $\Delta E_g \sim 3.0\text{ eV}$ [17]). The value of ΔE_g increases abruptly above 3 eV as the GaS thickness decreases to a monolayer due to quantum confinement effects [18]. Thus, according to its properties, GaS is between 2D-semiconductors with a small and insulators. This is of interest for the implementation of ultraviolet (UV) selective photoreceivers [19], adjusted by blue color/UV-light-emitting diode (LEDs) and heterojunctions in photocatalysis [20–22].

Creation of methods for inspect the defect structure of materials is an important task. Study of the impact of structure defects on physical and chemical properties of 2D-materials is important for the micro- and nano-electronics. Disordering of point defects, sizes of which are in the nanometer range, in crystalline materials is usually studied by experimental methods, e.g., dependences of properties on material composition and structure are studied. However, the aforesaid task in semiconductor compounds is complicated by the presence of defect orientation, nonequivalent cationic and anionic sublattices [23]. Restrictions on application of experimental methods lead to an ambiguous interpretation of defect nature and location.

Theoretical approaches are developing along with experimental studies of defects. Atomistic models, based on semiempirical parameterization of interatomic forces (interatomic potentials), thermodynamic and crystal-chemical approaches do not always allow for successful solving of

problems related to structure defects [24]. Interatomic potentials are usually created using a limiter set of parameters (cohesion energy, elastic constants and stacking-fault energies) that characterize a material. Thermodynamic methods presuppose availability of a database on energies of cation and anion formation and stabilization in certain crystallographic sites. Application of such approaches was often incorrect from the viewpoint of predicted formation and migration energies, as well as atomic configurations of defects.

Calculations based on the density functionality theory have significantly improved the quality of predictions of defect crystal properties. DFT calculations usually rely on the quantitative basis of modeling of atomic disordering in a solid body and take into account the influence of external impacts on the structure [25]. DFT calculations of defect structures are performed using the known computer programs. Modeling of properties makes it possible to estimate the defect nature, concentration, crystallographic disordering of atoms and defects. According to the results of *ab initio* calculations, e.g., in the paper [26], it was shown that the GaS band gap increases ($\Delta E_g \approx 3.325\text{ eV}$) as the number of GaS layers decreases.

Defect behavior in 2D-materials has been studied insufficiently, while defects may significantly affect surface states. The material surface state may also significantly affect the defect behavior. Various defect types may exist in semiconductor compounds, in particular, such as neutral and charged atomic vacancies, interstitial atoms, Schottky and Frenkel defects.

Many compounds of the $A^{III}B^{VI}$ type have a non-stoichiometric composition [3]. Therefore, for instance in GaS, sulfur and gallium deficits, which manifest themselves as point defects (vacancies) of sulfur and gallium, may affect the energy atomic configuration and conductivity ($\sigma_{\parallel} = 4 \cdot 10^{-13}\ \Omega^{-1} \cdot \text{cm}^{-1}$; $\sigma_{\perp} = 8 \cdot 10^{-8}\ \Omega^{-1} \cdot \text{cm}^{-1}$ at 400 K [4]). As is known, defects affect material properties. Therefore, the study of defects' interaction on the atomic scale is important for describing the electron and energy structure. Reactions between defects in an atomic lattice can be considered similarly to chemical reactions between molecules. This similarity is related to the fact that defects can be considered as quasiparticles characterized by their position, speed, mass and effective mobility [23].

Taking into account the aforesaid, it is currently important to choose DFT methods and modern models of interatomic forces when modeling the intermolecular interaction with defect participation [25]. The following two aspects of study of defect formation in crystals are important. Firstly, defects forming as a result of disruption of the structure crystalline lattice perfection are small and, consequently, inaccessible for direct experimental observation. Secondly, the simplified models of interatomic forces, used for defect modeling before the DFT methods became available, are not accurate and reliable enough. For instance, defect structure in body-centered cubic metals, predicted by means of empirical potentials, turned out to be incorrect. The description of

the nature of interaction between vacancies also turned out to be incorrect; the specified description differed from the one found later using the DFT methods.

Besides the specified on, there is still no *ab initio* information about the energy of vacancy formation and migration in compounds of the $A^{III}B^{VI}$ type. The goal of this paper is DFT calculation of structural and energy characteristics of atoms in GaS supercells having ordered point defects.

2. Experimental and calculation procedure

Synthesis of GaS. GaS polycrystals were synthesized using the method of chemical interaction of high-purity parent elements (Ga and S) in a vacuumized quartz vessel. According to the data of X-ray phase (XPA) and microscopic analyses, the GaS polycrystals consisted of a hexagonal phase. The X-ray diffraction patterns reveal peaks (002), (004) (006), (008) and (208) of the hexagonal β -phase of GaS. The GaS diffraction peaks corresponded to the parameters $a = 3.583 \pm 0.002 \text{ \AA}$, $c = 15.475 \pm 0.005 \text{ \AA}$ (Fig. 1) and the data of the JCPDS chart № 30-0576 for β -GaS (sp. gr. $P6_3/mmc$, (194), $a = 3.587 \text{ \AA}$ and $c = 15.492 \text{ \AA}$).

A monocrystal of the necessary GaS polytype with a stoichiometric composition is difficult to grow due to chalcogen volatility at growth temperatures ($< 1230 \text{ K}$). The GaS monocrystals were obtained by the Bridgman method [3]. The known data on GaS (JCPDS chart № 30-0576) was used as a reference of the structure for GaS. The GaS monocrystals grown by us showed high photoelectric and dielectric properties. The GaS monocrystals were yellow. These GaS samples become lighter after annealing at 1273 K for 5 h in vacuum. The GaS monocrystals grown with a relatively high growth speed ($> 2 \text{ mm/h}$) contained point defects. Structure defects affect the dielectric and electric properties of GaS [1,5].

Calculation procedure. The calculations were performed by the DFT method using pseudopotential plane waves [27–30]. The GaS supercells, containing 36 and 48 atoms, as well as vacancies of Ga and S atoms were used. Exchange-correlation energy was calculated by means of both a local density approximation (LDA) [27,28] and a generalized gradient approximation (GGA) [29] using the basic sets in different implementations. The values of the calculated parameter y_{ij} were taken as an average value for individual calculations of y_{ij} . The standard deviation was calculated using the formula $\sigma_i = \sqrt{\sum_j (y_{ij} - y_i)^2 / (n - 1)}$, where n is the total number of calculations [14,30].

The crystalline structure was optimized until the maximum value of the interatomic forces was less than 0.01 eV/\AA , while the maximum value of the mechanical stress tensor was less than 0.01 eV/\AA^3 .

A grid of $2 \times 2 \times 2$ k -dots, generated by a Monkhorst–Pack scheme, was used in DFT calculations with involvement of GaS supercells with Ga or S vacancies for

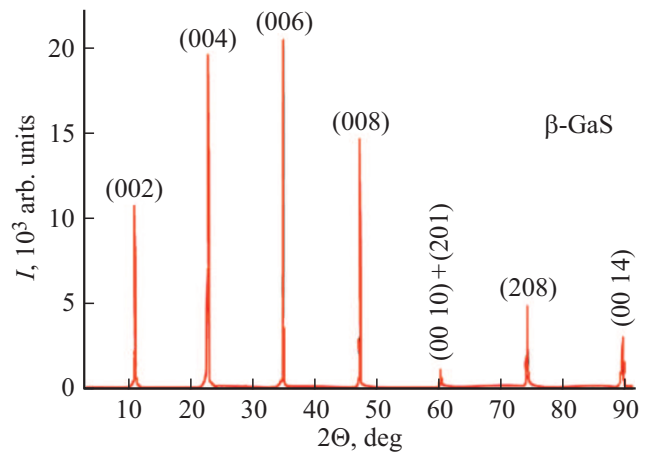


Figure 1. Diffraction pattern for a powder sample of GaS monocrystal at 298 K.

numerical integration by the Brillouin zone [31]. Kinetic cutoff energy E_{cut} that determines the plane wave sphere was 410 eV . The maximum value E_{cut} did not exceed 2040 eV [14,30].

Self-coordinated total energies were obtained using a density mixing scheme in combination with the conjugate gradient method. Atom positions were optimized by the Broyden–Fletcher–Goldfarb–Shanno algorithm (BFGS algorithm) [32]. Geometrical coordinates of atoms in a supercell were optimized taking into account the conjugate gradients by calculating the forces that act on atoms. Relaxation was performed by minimizing the forces acting on each atom. The GaS crystalline cell was optimized with a force tolerance equal to 0.01 eV/\AA and a voltage tolerance equal to 0.001 eV/\AA^3 .

Calculation of vacancy formation energy. In the DFT calculation, a defect in the shape of vacancy (V) forms by removing an atom from the lattice node in the supercell and weakening of the obtained atomic structure. Vacancy formation energy is generally calculated using the equation

$$E_f^V = E_{\text{tot}}^{N-1(\text{relaxed})} - \left(\frac{N-1}{N} \right) E_{\text{tot}}^{N(\text{perfect})}, \quad (1)$$

where $E_{\text{tot}}^{N-1(\text{relaxed})}$ is the supercell's total energy (relaxed) with removed one atom, $E_{\text{tot}}^{N(\text{perfect})}$ is the cell's total energy (perfect) with defect-free atoms. The indexes $N-1$ and N refer to the total quantity of atoms in a cell. This equation shows that determination of vacancy formation energy requires two separate DFT calculations. Finding a sufficiently accurate value of vacancy formation energy requires a relatively small cell containing less than 100 atoms.

Enthalpy of GaS hexagonal phase formation and energy of neutral vacancy formation in GaS supercells was calculated by the DFT method. Neutral atomic vacancies were formed in GaS supercells to determine vacancies' impact on the GaS properties. Energy of neutral vacancy formation was calculated. Formation enthalpy was calculated for a model

hexagonal structure of GaS that forms under atmospheric pressure. Energy of Ga and S vacancy formation in GaS was calculated using supercells containing 36 and 48 atoms. This quantity of Ga and S atoms is respectively in 4.5 and 5 times greater than the quantity of atoms in a GaS primitive cell.

Location of atoms around vacancies (Ga or S) in GaS supercells was optimized taking into account the relaxation of the first and second nearest neighbors of vacancy atoms. The parameters of the GaS crystalline lattice were fixed on the optimized value of an ideal crystal.

3. Calculation results and discussion

On the whole, the chemical bond between dissimilar atoms in solid bodies is covalent-ionic-metallic in nature. The contribution of covalent bond in semiconductors is always considerable. One of the criteria that a substance is a semiconductor is the prevalence of covalent contribution to the chemical bond. The contribution of ionic bond increases as the electronegativity difference increases. In GaS, the metallic component of the chemical bond is small, therefore the interatomic bond in GaS is covalent-ionic.

Let us assume that the following limitations are observed in a GaS crystal during defect formation. 1) The ratio of number of places in a sublattice is constant; 2) creation of places complies with the structure formula, i.e. when the number of atoms increases in one sublattice, a number of vacancies, proportional to the structural formula, arises in the other sublattice; 3) the mass balance is observed, i.e. the sum of element masses in the right and left members of quasi-chemical equations are equal; 4) electroneutrality is observed.

It was established that the obtained GaS monocystal has a high specific resistance ($\sigma_{\parallel} \approx 10^{-13} \Omega^{-1} \cdot \text{cm}^{-1}$; $\sigma_{\perp} \approx 10^{-8} \Omega^{-1} \cdot \text{cm}^{-1}$) and the band gap $\Delta E_g = 2.53 \text{ eV}$ at 300 K. Figure 2 shows the frequency dependences of ac-conductivity (alternating current conductivity) across the layers in the grown GaS monocystal up to (curve 1) and after electron irradiation (e^- -irradiation) with various doses (curves 2 and 3). As seen in Fig. 2, ac-conductivity of the GaS monocystal decreases as a result of e^- -irradiation. Electroconductivity decrease of irradiated semiconductors, as is known, is related to the compensation of the initially existing electrically active impurity centers by deeper energy levels of radiation defects. Conductivity compensation in semiconductors with deep energy levels of radiation defects can be pronounced. This phenomenon probably also occurs in a GaS monocystal. Thus, irradiation of the GaS monocystal causes radiation defects and stimulates the annealing and migration of defects existing in the crystal. This leads to an energy redistribution of local states in the Fermi level vicinity, due to which, as the dose of e^- -irradiation accumulates in the GaS sample, the energy band of the states, localized near the Fermi level, extends.

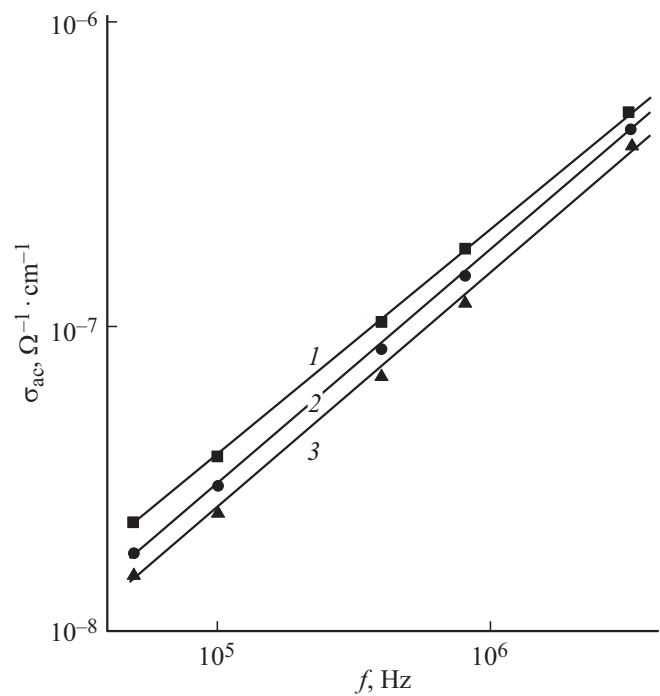


Figure 2. Ac-conductivity of GaS monocystal as a frequency function: before irradiation (1) and after e^- -irradiation with doses $2 \cdot 10^{12}$ (2) and 10^{13} cm^{-2} (3).

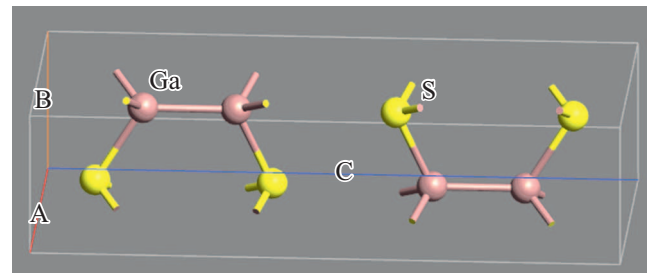


Figure 3. Primitive cell of the GaS compound.

3.1. Lattice parameters and band structure of the GaS supercell

The calculated parameters for the lattice of the GaS hexagonal phase were obtained at 0 K, while the experimental values were obtained at higher temperatures. However, the calculated lattice parameters in GaS reproduced the experimental values with the error of 2%. In other words, the DFT calculations for the GaS primitive cell (sp. gr. $P6_3/mmc$, (194)) have showed that the calculation data agree well with the experimental values (Table 1).

Calculations of the GaS band structure for the primitive cell (Fig. 3) in a local density approximation (LDA) have showed that the band gap (ΔE_g) is indirect and equal to $\Delta E_g = 1.57 \text{ eV}$ (Fig. 4, a). A comparison of the estimated value of ΔE_g for GaS with the experimental values of $\Delta E_g = 2.53 \text{ eV}$ [18] shows that they differ considerably.

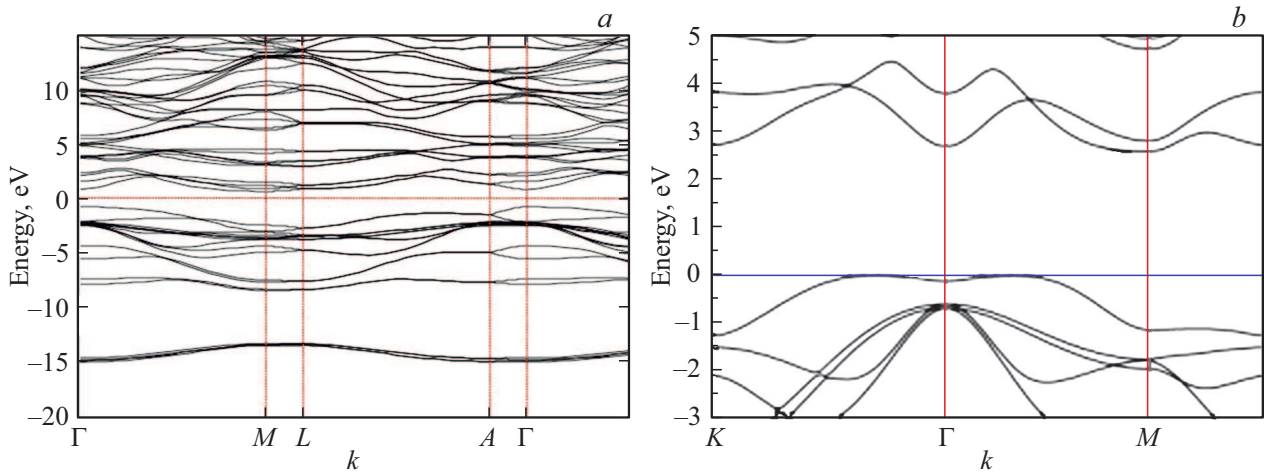


Figure 4. Band structure of the GaS compound primitive cell. a) — LDA approximation; b) — LDA + GGA approximation.

The band gap of GaS calculated by the DFT-LDA method (Fig. 4, a) turned out to be lesser than the experimentally obtained ΔE_g .

The use of non-hybrid functionalities in DFT calculations usually underestimates the calculated values of ΔE_g for semiconductors (the so-called „problem of band gap correction“) [33]. In compliance with this, we may assume that the filled narrow energy bands of the Ga 3d-state in GaS are strongly related to the S 2p-states obtained from

Table 1. Parameters of GaS lattice in hexagonal (sp.gr. $P6_3/mmc$) syngony obtained using exchange-correlation functions

Method	Parameters of lattice, Å	Error, %
GGA PBE (this paper)	$a = 4.002$ $c = 15.440$	0.3
LDA (this paper)	$a = 3.957$ $c = 15.268$	1.5
PBE [6]	$a = 3.630$ $c = 15.701$	1
PBE [8]	$a = 3.617$ $c = 15.496$	—
Experiment (this paper)	$a = 3.583$ $c = 15.475$	—
Experiment [1,18]	$a = 3.583$ $c = 15.475$	—
JCPDS chart № 30-0576	$a = 3.587$ $c = 15.492$	—
Experiment [3]	$a = 3.578$ $c = 15.47$	—
Experiment [7]	$a = 3.592$ $c = 15.495$	—
Reference book [4]	$a = 3.587$ $c = 15.492$	—

the sulfur 2p-orbitals. Then the Ga d-state can possibly be included as a valence state in GaS and it will affect the structural parameters, change the energy band and deformation potential. Otherwise, i.e. if we neglect the Ga 3d-states in GaS, then the 3d-states will be considered as frozen-nucleus states.

The estimated value of ΔE_g for the GaS compound was agreed with the experimental ΔE_g . Exchange energy was calculated taking into account the contributions of exchange energy and electron correlation to the expression of electron density functionality. Estimation also took into account the small influence of the Ga d-state on the GaS band gap. The exchange-correlation potential was calculated by the GGA-PBE method. The obtained result of calculation of $\Delta E_g \approx 2.50$ eV agrees well with the experimental $\Delta E_g = 2.53$ eV [18]. The calculated lattice parameters and ΔE_g for GaS agree with the experimental values within the error $\leq 3\%$, typical for DFT-calculations. A hybrid variant of the DFT method was used to calculate the total energy in the paper [9]

$$E_{\text{tot}}^{\text{hyb}}(1-x)E_X^{\text{HF}} + xE_X^{\text{DFT}} + E_C^{\text{DFT}}, \quad (2)$$

where $E_{\text{tot}}^{\text{hyb}}$ is the total energy obtained by the hybrid DFT method, $1-x$ is the energy fraction obtained by calculation using the Hartree-Fock method (HF) in the functionality, E_X^{HF} is the contribution of exchange energy under the HF method, E_X^{DFT} is the contribution of exchange energy in the non-hybrid (simple) DFT variant, E_C^{DFT} is the contribution of correlation energy in the non-hybrid DFT variant. It was stated that the DFT-calculations (containing 13% of exchange as per Hartree-Fock) were performed using the exchange-correlation functionality of PBE. The indirect band gap for a GaS monolayer is 3.30 eV, which is considerably larger than the corresponding value for bulk crystals.

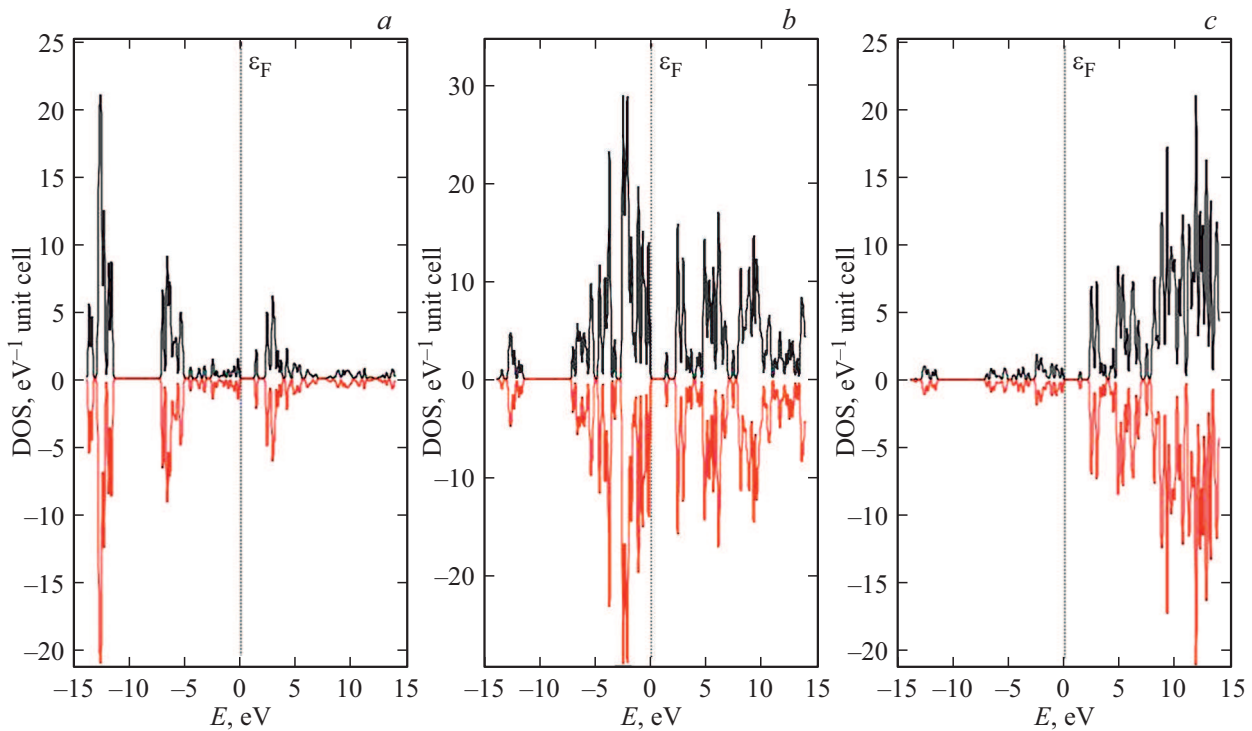


Figure 5. Density of states (DOS) for a GaS supercell containing a Ga-vacancy (model $\text{Ga}_{17}\text{S}_{18}$) with an up spin (black) and down spin (red). *a*) *s*-state, *b*) *p*-state, *c*) *d*-state.

3.1.1. Electron structure of GaS supercell

It follows from the general approach to covalent bond description that the wave function Ψ of an electron pair in the molecular orbital method (MOM) is characterized by overlapping of individual fragments' wave functions. Interaction of an undivided electron pair in an atom of one GaS molecule will be considered within the framework of MOM. Let us assume that the wave function Ψ for a GaS semiconductor is characterized by orbital approximation and linear combination of atomic orbitals: $\Psi_{\text{GaS}} = a\Psi_{\text{Ga}} + b\Psi_{\text{S}}$, where Ψ_{Ga} and Ψ_{S} are wave functions involved in the atoms' chemical bond, coefficients $a \neq b$ are the share of each atom's involvement in the quantum-chemical bond. The electron density maximum in each GaS covalent bond will be shifted towards an atom having a higher electronegativity, i.e. electron clouds in GaS will be tied to the crystalline lattice nodes where sulfur atoms are located.

Thus, the chemical bond in GaS 2D-crystals between the orbitals of Ga $4p$ and S $3p$ can be considered to be heteropolar covalent. Thereat, the electron density is redistributed near the nuclei that form a GaS molecule. Then lattice nodes will contain neutral atoms, and the bond between them will be via electron pairs. A covalent bond is known to have a directional pattern and to form in the direction where the density of an electron cloud of paired electrons is the largest. Therefore, it can be assumed that each crystalline lattice atom in GaS may interact only with certain atoms, and not with all atoms as in ionic crystals.

Given the aforesaid and the quantum chemistry theory, the GaS valence band must consist of bonding atomic orbitals S $3p$ and Ga $4p$ ($\Psi_+ = \Psi_b = \Psi_{\text{Ga}} + \Psi_{\text{S}}$ bonding MO), where the valence band top consists of the orbital of the S component $3p$. On the other hand, the GaS conductivity band will consist of antibonding orbitals of Ga $4p$ and S $3p$ ($\Psi_- = \Psi_a = \Psi_{\text{Ga}} - \Psi_{\text{S}}$ antibonding MO), while the conductivity band bottom includes nonbonding orbitals which arise due to the atomic orbitals of the Ga component $4p$.

3.2. Ga vacancy in a 36-atom GaS supercell (model $\text{Ga}_{17}\text{S}_{18}$, where indexes show quantity of the corresponding atoms)

Nonstoichiometry, i.e. violation of stoichiometric ratio between atoms in compounds, in particular, metal chalcogenides (MCh) [3], causes a change in defect formation in the MCh volume. Point defects in a crystal usually form during material growth, plastic deformation and heat treatment. Degree of MCh nonstoichiometry is changed by electric properties of the material based on MCh. Semiconductor chalcogenide materials are subdivided into two conductivity types, *p*-type and *n*-type, related to a metal deficit (or excess) or to chalcogen shortage (or excess) [3]. Let us assume that vacancies in a GaS crystal act as donors if quantity of unpaired electrons near a vacancy is less than half of the quantity of valence electrons, existing in a similar place of a perfect crystal, and otherwise as acceptors.

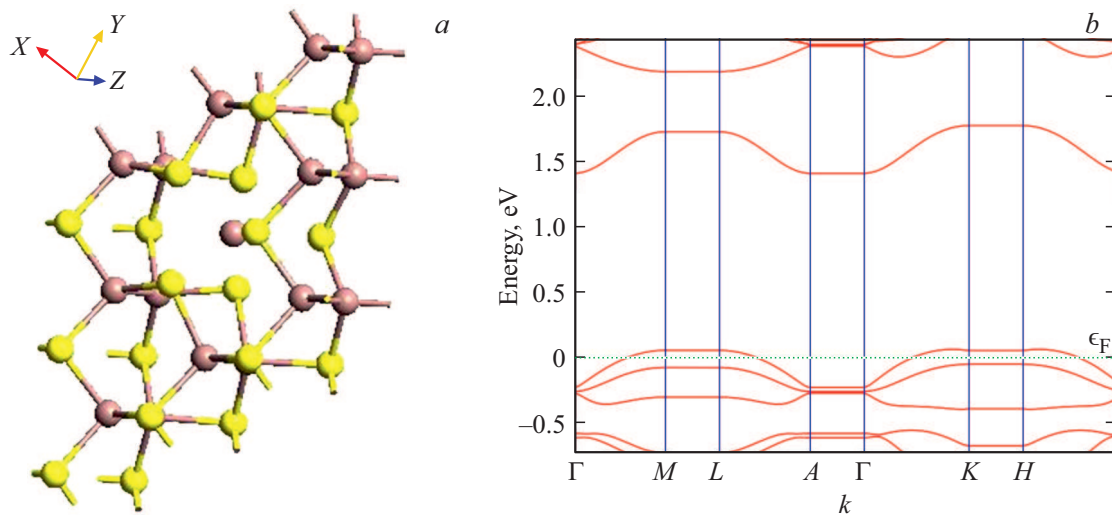


Figure 6. Atomic (*a*) and band structure (*b* — LDA approximation) of a 36-atom GaS supercell with a Ga vacancy (model $\text{Ga}_{17}\text{S}_{18}$).

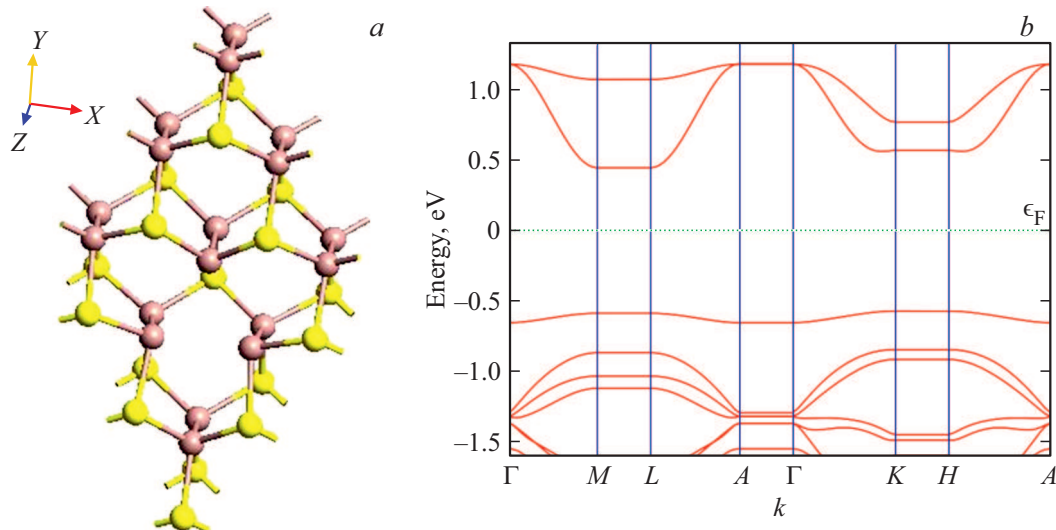


Figure 7. Atomic (*a*) and band structure (*b* is LDA approximation) of a 36-atom GaS supercell with an S vacancy (model $\text{Ga}_{18}\text{S}_{17}$).

Then a chiefly covalent bond is created in the GaS crystal between Ga and S by means of eight valence electrons. With this bond of GaS atoms, outer electrons of two neighboring atoms will pair up, forming common orbits around both atoms (Ga and S), thereat, spins in each pair are antiparallel owing to the Pauli principle. In a GaS crystal, e.g., with a gallium vacancy Ga (V_{Ga}), where V_{Ga} will be surrounded by unpaired electrons of sulfur atoms, it can accept electrons for bonding with them. Thereat, V_{Ga} may charge negatively and act as an acceptor. On the contrary, a sulfur vacancy surrounded by unpaired electrons of gallium atoms will be a donor.

A semiconductor of the *p*-type with a metal deficit, e.g., such as a GaS crystal, can be represented as Ga_{1-x}S (*x* is the atomic fraction), where the crystal has a set of atomic defects for any non-zero value. Then in case of $x > 0$

the crystal will have metal vacancies V_{Ga} , while in case of $x < 0$ the crystal will have additional Ga atoms, located at interstitial positions Ga_i . I.e. charged vacancies F_{Ga} will be the predominant defects in sulfur-rich GaS crystals. The GaS_{1-x} crystal will contain vacancies of ionized sulfur and gallium interstitial sites.

During defect formation, positively and negatively charged defects, defect complexes, free electrons or their vacancies may form in GaS. The electroneutrality condition shall be ensured by formation of an equal quantity of positively and negatively charged defects. Let us consider the GaS supercells having neutral point defects (Ga and S vacancies) in the corresponding sublattices.

Figures 5 and 6 give the calculated densities of electron states (DOS), the atomic and band structures of the GaS supercell with a gallium vacancy (model $\text{Ga}_{17}\text{S}_{18}$).

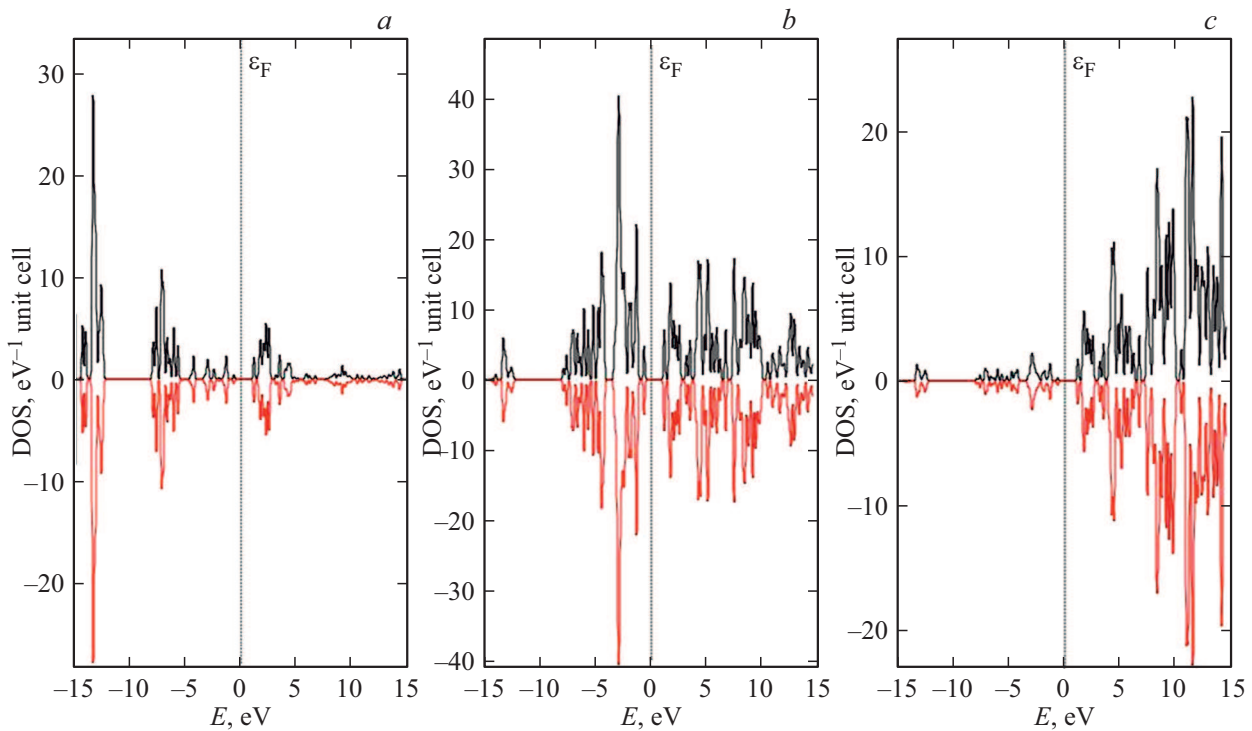


Figure 8. Density of states (DOS) for a GaS supercell containing an S vacancy (model $\text{Ga}_{18}\text{S}_{17}$) with an up spin (black) and down spin (red). *a)* *s*-state, *b)* *p*-state, *c)* *d*-state.

The results of the calculations of electron state density in a 36-atom GaS supercell with an ordered Ga vacancy (model $\text{Ga}_{17}\text{S}_{18}$) at the specified lattice parameters (hexagonal, $a = 4.002 \text{ \AA}$, $c = 15.440 \text{ \AA}$, sp.gr. $P6_c/mmc$, (194)) are given in Fig. 5.

Figure 6 gives the atomic (6, *a*) and band structures (6, *b*) of the GaS supercell with a gallium vacancy, more precisely the model of the $\text{Ga}_{17}\text{S}_{18}$ supercell. It follows from Fig. 6, *b* that the band structure of GaS with a Ga vacancy has an indirect band.

3.3. S vacancy in a 36-atom GaS supercell (model $\text{Ga}_{18}\text{S}_{17}$)

Figures 7, *a* and 7, *b* give the atomic and band structures in a 36-atom GaS supercell with an S vacancy (model $\text{Ga}_{18}\text{S}_{17}$) (hexagonal, $a = 4.002 \text{ \AA}$, $c = 15.440 \text{ \AA}$, sp.gr. $P6_3/mmc$, (194)). Presence of an S vacancy causes a decrease in ΔE_g . The $\Gamma \rightarrow K$ band in Fig. 7, *b* is indirect.

Figure 8 shows the densities of electron states of a 36-atom GaS supercell with an S vacancy. It follows from the analysis of *s*-, *p*- and *d*-states of DOS that the spin up and spin down states for the $\text{Ga}_{18}\text{S}_{17}$ supercell are symmetrical.

3.4. Ga vacancy in a 48-atom GaS supercell (model $\text{Ga}_{23}\text{S}_{24}$)

The geometry of the atom structure in the GaS supercell with a Ga vacancy was modeled (model $\text{Ga}_{23}\text{S}_{24}$)

(hexagonal, $a = 3.585 \text{ \AA}$, $c = 15.500 \text{ \AA}$, sp.gr. $P6_3/mmc$, (194)). It was found that the bond lengths between two neighboring Ga-Ga, Ga-S atoms differ considerably from each other. Bond lengths, for instance, for the specified atoms $\text{Ga}_{10}\text{-Ga}_{21}$, $\text{Ga}_{11}\text{-S}_{22}$, are $d_{\text{Ga}_{10}\text{-Ga}_{21}} = 2.47 \text{ \AA}$, and $d_{\text{Ga}_{11}\text{-S}_{22}} = 2.37 \text{ \AA}$ respectively.

3.5. Energy (enthalpy) of GaS formation

Stability of a defect in the crystalline lattice of a substance is determined by two factors: energy (as a result of system's striving to the free energy minimum) and geometry (as fulfillment of certain ratios between effective defect sizes and the corresponding place in the crystalline lattice). A change in enthalpy of formation one mole of a given chemical compound from the contained chemical elements in their standard states at temperature T K and the standard pressure of 1 atm (101.3 kPa) is expressed as

$$\Delta_f H_T^\circ = \Delta_f H_0^\circ + \int_0^T \Delta C_p dT \quad (3)$$

where $\Delta_f H_T^\circ$ is the standard enthalpy of substance formation at 0 K, ΔC_p is the molar heat capacity of a substance at a constant pressure ($p = \text{const}$). (A standard state of a substance is a state when a substance is in the most stable form under the standard pressure.) Taking this into account, the standard enthalpy of GaS formation at temperature T

Table 2. Theoretical and experimental enthalpies of GaS phase formation in a hexagonal structure

Phase	Formation enthalpies, $-\Delta_f H_{298}^\circ \text{GaS}$, kJ/mol		
	Calculation	Experiment	
GaS ($P6_3/mmc$)	188.4	194.1 ± 14.6	[36] (EMF measurement)
		209.2 ± 20.9	[35] (calorimetry)
		196.2	[3]

was calculated using the equation

$$\begin{aligned} \Delta_f H_T^\circ(\text{GaS}) &= H_T^\circ(\text{GaS}) - H_T^\circ(\text{Ga}) - H_T^\circ(\text{S}) \\ &+ \int_0^T [C_p(\text{GaS}) - C_p(\text{Ga}) - C_p(\text{S})] dT \\ &\approx \Delta_f H_0^\circ(\text{GaS}) = \Delta_f U_0^\circ(\text{GaS}) \\ &= E_{\text{tot}}^\circ(\text{GaS}) - [E_{\text{tot}}^\circ(\text{Ga}) + E_{\text{tot}}^\circ(\text{S})] \end{aligned} \quad (4)$$

where $\Delta_f H_T^\circ$ is the standard enthalpy of GaS formation, $\Delta_f U_0^\circ$ is the change in internal energy, E_{tot}° is the total standard energy of a compound per formula unit of GaS. Here, the formation enthalpies of simple substances ($H_T^\circ(\text{Ga})$ and $H_T^\circ(\text{S})$) are equal to zero. Taking into account the reference data [4,34,35], the equation $C_p(\text{GaS}) = 41.4 + 15.7 \cdot 10^{-3} \cdot T \text{ J}/(\text{mol} \cdot \text{K})$ has been obtained for GaS. The molar heat capacity estimated by the Neumann-Kopp method does not greatly differ from the sum of atomic heat capacities of the elements $C_p(\text{Ga}) = 26.1$ and $C_p(\text{S}) = 22.6 \text{ J}/(\text{mol} \cdot \text{K})$ at 298 K [35]. Taking this into account, the contribution to the equation (2) in calculations of GaS formation energy was taken equal to zero. In this case, GaS formation enthalpy can be expressed as a change in internal energy $\Delta_f U_0^\circ(\text{GaS})$.

The values of GaS formation enthalpy, calculated using the formula (4) and obtained experimentally, are given in Table 2. Theoretical formation enthalpy $\Delta_f H_T^\circ(\text{GaS}) = -1.95 \text{ eV}$ was obtained for the hexagonal phase. This calculated value ($\Delta_f H_T^\circ(\text{GaS}) = -188.4 \text{ kJ/mol}$) corresponds to reference experimental data ($\Delta_f H_{298}^\circ = -196.2 \text{ kJ/mol}$ [3]; $-209.2 \pm 20.9 \text{ kJ/mol}$ [35]; $-194.1 \pm 14.6 \text{ kJ/mol}$ (EMF measurement) [36]; -187.4 kJ/mol (calorimetry) [36]), according to which the hexagonal phase is stable at room and low temperatures.

3.6. Geometry around Ga and S vacancies in GaS supercell

Let us consider the results of optimization of the atoms' nearest neighbors around the GaS supercell vacancy consisting of 48 atoms. A comparison of distances between the vacancy and neighbor atoms before and after geometry optimization has revealed shifts of the neighboring atoms, accompanied with Ga and S vacancies (Table 3). Analysis of

Table 3. Distance between a vacancy and neighbor atoms before and after geometry optimization and shift of neighbor atoms with Ga and S vacancies

Bond between vacancy and atoms	Distance between vacancy and atoms		
	l_{befor}^a	l_{after}^b	Δl^c
	Å		
$V_{\text{Ga}}-\text{S}$	2.875	2.885	+0.01
$V_{\text{Ga}}-\text{Ga}$	2.411	2.377	-0.03

Note. a) Atomic distance before geometry optimization. b) Atomic distance after geometry optimization. c) Shift of neighboring atoms.

distances between Ga and S vacancies and neighbor atoms before and after geometry optimization made it possible to draw the following conclusion.

1. In case of formation of a Ga atom vacancy in a GaS supercell, bonds between the Ga atom and the surrounding S atoms are broken. As a result, atoms of the S nearest neighbors migrate away from the Ga vacancy. The neighboring atoms of Ga move in a direction that approaches the Ga vacancy position. Assuming that the Ga-S bond is covalent, then when a Ga becomes vacant, it will affect the electron structure of coordinated S atoms.

It follows from the analysis of state density of the GaS supercell with Ga vacancies that the main component of the valence band top is an S orbital $3p$, therefore the acceptor level in the band gap must be created on top of the valence band.

2. In case of an S atom vacancy in the GaS supercell, bonds between the S atom and the neighboring Ga atoms break. As a result, the neighboring Ga atoms migrate away from the vacancy. S atoms of a vacancy neighbor move in the direction which approaches the S vacancy position. As in the case (1), when an S crystalline node contains a vacancy, this affects the Ga electron structure. Therefore, state density of Ga atoms of the vacancy's nearest neighbor changes in a greater extent that the DOS atoms of the nearest neighbor of Ga in the GaS supercell. DOS analysis of the GaS supercell with S vacancies shown that a component in the lower conductivity band is the $4p$ -orbital of Ga, which creates a donor level under the lower part of the conductivity band.

3. The value of offset of the nearest neighboring atoms of the GaS supercell with Ga and S vacancies, obtained as a result of generation of a Ga vacancy ($\Delta l(V_{\text{Ga}} - \text{S})$), is 0.01 Å, while the shift value determined by generation of an S vacancy ($\Delta l(V_{\text{S}} - \text{Ga})$) is 0.03 Å. In other words, the impact of an S vacancy on the surrounding atoms in GaS is lesser than the impact of the Ga vacancy.

3.7. Energies of Ga and S vacancy formation in GaS. Chemical potential

Structure-susceptibility properties (electrical conductivity, optical properties, luminescence etc.) of a GaS semiconductor crystal heavily depend on the impact of impurities and defects [5]. The degree of change in these properties is determined by defect concentration and type. One of the main parameters that characterize a point defect is the defect formation energy E_f^{def} .

The process of Ga and S vacancy formation in the GaS supercell can be classified as a homogeneous open thermodynamic system, where system weight and composition change due to substance withdrawal or addition, or owing to occurrence of a chemical reaction. The system state functions in open thermodynamic systems, namely the internal energy U , enthalpy H , Helmholtz energy F and Gibbs energy G are also a function of the quantity of individual components that make up a given system. Removal of some amount of the substance from an open system or its appearance in a system will affect the system's internal energy reserve.

In isochoric- (or isobaric)-isothermal conditions, increment of the Helmholtz free energy (ΔF) or Gibbs energy (ΔG) of an open system upon addition of one mole of the given component is equal to chemical potential μ_i . Chemical potential is determined by one of the following partial derivatives:

$$\begin{aligned}\mu_i &= (\partial U / \partial n_i)_{S,V,n_{j \neq i}} = (\partial H / \partial n_i)_{S,P,n_{j \neq i}} \\ &= (\partial F / \partial n_i)_{V,T,n_{j \neq i}} = (\partial G / \partial n_i)_{P,T,n_{j \neq i}},\end{aligned}$$

where n_i is the number of moles of all components, except the component, the change of which is under consideration. The value of μ_i characterizes the degree of change in total energy, in particular, Gibbs free energy ΔG of a system with $T = \text{const}$, $P = \text{const}$ and addition of an infinitely small amount of component i without a change in the number of moles of the other components j . I.e. in this case the amount of the other substances in the given system per mole remains constant. Therefore, chemical potential of the i -th component coincides with the partial isobaric potential ($\mu_i = \overline{G}_i$) of one mole of a substance. In other words, it is assumed that an open system is so large that its composition upon addition of one mole of the i -th component virtually does not change.

On the other hand, chemical potential of the i -th component is determined by a known ratio: $\mu_i = \mu_i^0 + RT \ln(x_i)$ or

$\mu_i = \overline{H}_i^0 - T\overline{S}_i^0$, where μ_i^0 is the standard chemical potential of the i -th component in the pure phase, R is the universal gas constant, \overline{H}_i^0 and \overline{S}_i^0 are standard molar partial enthalpy and entropy. From here it follows that the atom's chemical potential changes depending on chemical composition. In particular, value of μ_i in a GaS supercell with a vacancy must depend on composition of the GaS compound.

Let us consider the relation of the defect formation energy E_f^{def} to the system's free energy in the course of formation of n (number of defects in the crystal). System's work in an isothermal reversible process is equal to the decrease of ΔF ($V = \text{const}$) or ΔG ($P = \text{const}$). On the other hand, E_f^{def} is determined by the work for atom transfer from a crystalline lattice node to the crystal surface. Formation of point defects in thermodynamic equilibrium conditions will increase crystal entropy (S). Thereat, n atoms can be removed from a crystal, containing N identical atoms, by various methods. I.e. n number of defects ($n \ll N$) can be created in a crystal composed of N atoms at N crystal positions (number of molecules in 1 mole $N_A = 6.02 \cdot 10^{23}$ — Avogadro number). Then, according to the Boltzmann formula, the corresponding change in configuration entropy is equal to: $\Delta S_c = k_B \ln W = k_B \ln \left[\frac{N!}{n!(N-n)!} \right]$, where k_B is the Boltzmann constant. Here, $k_B T$ characterizes the energy of a „thermal“ quantum, equal to 0.026 eV at 298 K. In the equilibrium case, formation of an n -th number of defects at temperature T will change ΔF or ΔG of the crystal in compliance with the Gibbs–Helmholtz equation for the process: $\Delta F = n\Delta_f U^{\text{def}} - T\Delta S$ or $\Delta G = n\Delta_f H^{\text{def}} - T\Delta S$, where $\Delta S = S_c + nS_v^{\text{def}}$ (change in vibrational entropy upon formation of one defect). Here, $\Delta_f U^{\text{def}} \approx \Delta_f H^{\text{def}} = E_f^{\text{def}}$ is the energy (enthalpy or heat) of formation of one defect. From here it follows that $\Delta_f H^{\text{def}}$ with small n is small. A considerable contribution of $T\Delta S$ is determined by increase in configuration entropy $\Delta S_c = k_B \ln W$.

Minimization of ΔF or ΔG taking into account ΔS and factorials of number $\ln(n!) \approx n \ln(n)$ makes it possible to estimate the equilibrium number of point defects $n = N \exp(-\Delta_f H^{\text{def}}/k_B T)$, as well as equilibrium concentration of defects $C^{\text{def}} = \exp(S_v/k_B) \cdot \exp(-\Delta_f H^{\text{def}}/k_B T)$. Entropy contributions to the defect formation energy were neglected in the calculations. Firstly, we used supercells with monovacancies where the total defect concentration is significantly below 10^{-4} , while configuration entropy per defect is more than $10k_B$ and S_c^{def} , therefore, it can be the predominant contribution of entropy at high temperatures. Secondly, consideration of insignificant contributions by vibrational and magnetic entropy increases the computational costs by several efforts as compared to a static ($T = 0$ K) defect calculation. Energy of defect formation in a charge state q is equal to [37]:

$$E_f^{\text{q,def}} = E_{\text{tot}}^{\text{def}} - E_{\text{tot}}^{\text{bulk}} + \sum_i n_i \mu_i + q(E_F + E_{\text{VBM}}) + Q_c, \quad (5)$$

where $E_{\text{tot}}^{\text{def}}$ is the total energy of a supercell containing a defect, $E_{\text{tot}}^{\text{bulk}}$ is the total energy of a bulk supercell,

μ_i is the chemical potential of particles i added ($n_i > 0$) or removed ($n_i < 0$) from a cell to create a defect, E_F is the Fermi energy, E_{VBM} is the maximum of a valence band in the volume, so that $E_F \geq 0$, Q_c is electrostatic corrections to take into account the long-range electrostatic interactions of charged defects in neighboring supercells. Value of μ_i affects the defect formation energy, but not the energy levels of particles' transition. Defect ionization level, characterizing the degree of thermodynamic transition between the charge states q_1 and q_2 is determined as [37]:

$$\epsilon(q_1/q_2) = \frac{E_F^{q_1}|_{E_F=0} - E_F^{q_2}|_{E_F=0}}{q_1 - q_2}, \quad (6)$$

where $E_F^q|_{E_F=0}$ is the energy of defect formation in charge state q estimated at $E_F = 0$. Let us assume that $q = 0$ and the electroneutrality condition in GaS is ensured by formation of neutral vacancies of own Ga and S atoms. Formation energy $\Delta_f H^V$ or E_f^V of neutral vacancies of gallium (V_{Ga}^X) and sulfur (V_S^X) in the corresponding sublattices of GaS supercell was calculated using the following expressions [30]:

$$E_f^{V_{Ga}^X} = E_{tot}^{V_{Ga}^X+bulk}(Ga_{n-1}S_n) - E_{tot}^{bulk}(Ga_nS_n) + \mu_{Ga}, \quad (7a)$$

$$E_f^{V_S^X} = E_{tot}^{V_S^X+bulk}(Ga_nS_{n-1}) - E_{tot}^{bulk}(Ga_nS_n) + \mu_S, \quad (7b)$$

where $E_{tot}^{V_{Ga}^X+bulk}$ is the total energy for a supercell of a bulk substance having a neutral gallium or sulfur vacancy ($V_{Ga,S}^X$), E_{tot}^{bulk} is the total energy for a supercell of a bulk substance without a neutral vacancy, n is the number of atoms in the GaS supercell, μ_i is the chemical potential of i -th component.

Let us consider the dependence of μ_i on composition in GaS. We assume that, like other chalcogenide compounds of type $A^{III}B^{VI}$ [3], GaS has a small deviation from stoichiometry, i.e. it has a non-stoichiometric composition. Then the formation of solid Ga_xS_{x-1} or $Ga_{x-1}S_x$ solutions will be accompanied with a change in Gibbs free energy (ΔG). The following can be written for the mixing energy ΔG of one solution mode: $\Delta G = x_{Ga}\mu_{Ga} + x_S\mu_S$, where x_i is the molar fraction of component i in the solution.

The following equation shall be followed for the stoichiometric composition of GaS: $\mu_{Ga} + \mu_S = \mu_{GaS(bulk)}$, where $\mu_{GaS(bulk)}$ is the chemical potential for the GaS bulk compound. If we assume that the GaS composition insignificantly deviates from stoichiometry, then values of atoms' chemical potentials in the region of GaS homogeneity must be coordinated. For this purpose, the imaging points (compositions) for calculation of atoms' μ_i were chosen from the $T-x$ phase diagram of the Ga-S system [3,36].

The revised $T-x$ diagram for Ga-S is given in Fig. 9. On the solidus line of the $T-x$ diagram near the GaS compound, in addition to the stoichiometric composition, we chose one composition of $Ga_{0.501}S_{0.499}$ on the left and $Ga_{0.499}S_{0.501}$ on the right of the GaS stoichiometric composition, for which μ_i was calculated. The chosen

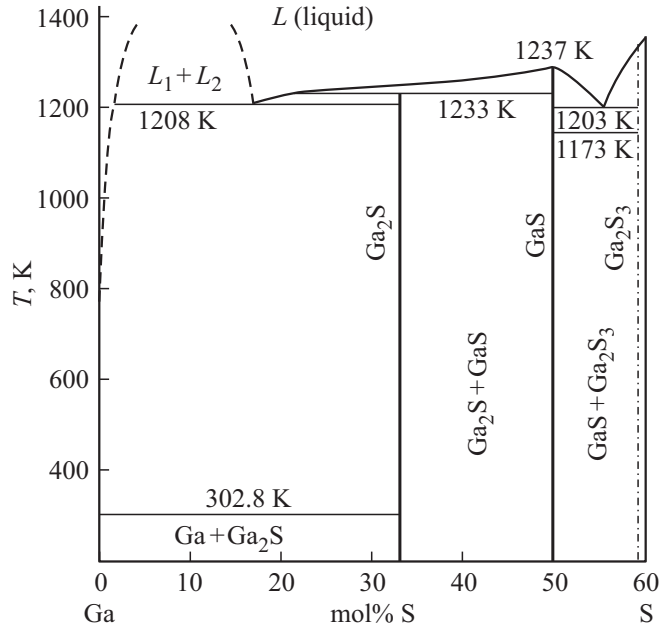


Figure 9. Phase diagram of Ga-S system state in the sulfur concentration interval of 0–60 at.%.

compositions on the $T-x$ diagram of Ga–S characterize the GaS equilibrium in heterogeneous regions of Ga_2S -GaS and GaS- Ga_2S_3 with compounds Ga_2S and Ga_2S_3 , respectively.

Based on the aforesaid and taking into account the $T-x$ diagram, Ga-S for the stoichiometric composition of GaS, the chemical potential of Ga and S atoms can be specified as follows:

$$\mu_{Ga} = [\mu_{Ga_2S(bulk)} - \mu_{GaS(bulk)}], \quad (8a)$$

$$\mu_{Ga} = [3\mu_{GaS(bulk)} - \mu_{Ga_2S_3(bulk)}], \quad (8b)$$

$$\mu_S = \mu_{S(bulk)}. \quad (8c)$$

Chemical potentials of bulk substances (GaS, Ga_2S and Ga_2S_3) in these equations were calculated as total energies per formula unit by way of separate calculations: $\mu_{GaS} = 4.9$ eV, $\mu_{Ga_2S} = 7.3$ eV, $\mu_{Ga_2S_3} = 12.9$ eV. Our DFT-calculated values of μ_{Ga} and μ_S differ by ~ 0.02 eV from the reference values of $\mu_{Ga} = 2.42$ and $\mu_S = 2.45$ eV [38] in the elements' gas state. Changes in μ_i of compounds $Ga_{0.501}S_{0.499}$ and $Ga_{0.499}S_{0.501}$ in the chosen region of GaS homogeneity are also within the error of ~ 0.02 eV. Taking into account μ_i for the substances (GaS, Ga_2S and Ga_2S_3), the calculated energies of Ga and S vacancy formation in GaS supercells were as follows: $E_f^{V_{Ga}^X} = 0.57$ and $E_f^{V_S^X} = 0.62$ eV.

Energy of Ga vacancy formation in GaS is lesser than energy of S vacancy formation. I.e. since energy of S vacancy formation in the GaS compound is more than ($E_f^{V_S^X} > E_f^{V_{Ga}^X}$), then the occurrence of an S vacancy is hindered. This agrees with the fact that when GaS polycrystals are synthesized directly by melting of stoichiometric amount of Ga and S in vacuum, Ga vacancies are easily created. On the

other hand, energy of S vacancy formation in conditions of sulfur shortage ($\text{Ga}_n\text{S}_{n-1}$) is ~ 0.62 eV. Consequently, an S vacancy can be easily generated for $\text{Ga}_n\text{S}_{n-1}$. An S vacancy in GaS can be eliminated by heat treatment in oxidation atmosphere at temperatures of ≤ 1100 K. The synthesized high-density GaS polycrystals after annealing in oxidation atmosphere, i.e. in an insignificant sulfur excess, had a stoichiometric composition. Energy of Ga vacancy formation is maximum both in sulfur-rich compositions and in the stoichiometric composition of GaS.

In GaS with a point defect (vacancy), we will consider the dependence of defect formation energies E_f^V on chemical potential μ . Value of E_f^V and, consequently, the equilibrium concentration of defects largely depends on atomic chemical potentials of S and Ga, as well as on chemical potential of electrons in a thermodynamically permitted range. Let us apply the following limitations on chemical potentials in conditions of equilibrium and electroneutrality for calculation of E_f^V in the GaS volume. If a system contains an excess of sulfur, such excess of S may deposit in the GaS volume. Consequently, the chemical potential of an excess of S cannot exceed the chemical potential of sulfur in the volume, i.e. $\mu_{\text{S(excess)}} \leq \mu_{\text{S(bulk)}}$. In the same way, the chemical potential of an excess of Ga cannot exceed the chemical potential of gallium in the volume $\mu_{\text{Ga(bulk)}}$, i.e. $\mu_{\text{Ga(excess)}} \leq \mu_{\text{S(bulk)}}$. Moreover, the sum of S and Ga chemical potentials must be equal to the chemical potential (per pair) of bulk GaS:

$$\begin{aligned} \mu_{\text{S}} + \mu_{\text{Ga}} &= \mu_{\text{GaS(bulk)}} \\ &= \mu_{\text{Ga(bulk)}} + \mu_{\text{S(bulk)}} - \Delta_f H(\text{GaS(bulk)}), \end{aligned} \quad (9)$$

where $\Delta_f H$ is the enthalpy of GaS formation.

In other words, the use of the above-mentioned limitations for an individual μ_i , which is set by the bulk elements S and Ga reveals that the GaS surface may be in equilibrium with the system's environment only if chemical potentials are within both the upper and the lower limits.

$$\mu_{\text{S(bulk)}} - \Delta_f H \leq \mu_{\text{S}} \leq \mu_{\text{S(bulk)}}, \quad (10a)$$

$$\mu_{\text{Ga(bulk)}} - \Delta_f H \leq \mu_{\text{Ga}} \leq \mu_{\text{Ga(bulk)}}. \quad (10b)$$

Thus, each μ_i is limited by a range which is by ~ 2 eV ($-\Delta_f H(\text{GaS}) = 2.17$ eV [35]; 1.97 eV [36], 2.03 eV [3]) lower than its corresponding volumetric value. These conditions limit the difference of chemical potentials $\mu_{\text{Ga}} - \mu_{\text{S}}$, by the range, which is determined by the heat of formation $\Delta_f H$ of bulk GaS from elementary S and Ga. Taking into account the given conditions, energy of defect formation E_f^V in a GaS supercell with one defect (vacancy) can be written as

$$E_f^V = E_D - n_e \mu_e - n_{\text{Ga}} \mu_{\text{Ga}} - n_{\text{S}} \mu_{\text{S}}, \quad (11)$$

where E_D is the energy of a supercell that contains n_{Ga} atoms of Ga, n_{S} atoms of S and one defect (vacancy). Here, n_e is the number of electrons carried over from the systems' electron reservoir (i.e. the system consists

of an arbitrarily large number of particles) with chemical potential μ_e into the defect for the given charge state.

Having defined that

$$\Delta\mu = (\mu_{\text{Ga}} - \mu_{\text{S}}) - (\mu_{\text{Ga(bulk)}} - \mu_{\text{S(bulk)}}) \quad (12)$$

we rewrite the value of E_f^V as

$$E_f^V = E_D - n_e \mu_e - \frac{1}{2} (n_{\text{Ga}} - n_{\text{S}}) \Delta\mu, \quad (13)$$

where E_D does not depend on $\Delta\mu$ and μ_e .

For an ideal crystal of a substance, the value of $E_D^{\text{id}} = 0$, and energy of formation $\Delta_f H$ of the substance becomes zero. For bulk GaS, if we apply the limitations on chemical potentials $0 \leq \mu_e \leq E_g$ and $-\Delta_f H \leq \Delta\mu \leq \Delta_f H$, where E_g is the band gap, then the GaS formation heat will be equal to $\Delta_f H = -(\mu_{\text{GaS}} - \mu_{\text{Ga(bulk)}} - \mu_{\text{S(bulk)}})$. In such calculations we can ignore the temperature dependence of E_D , E_g and $\Delta_f H$. However, the temperature dependence is significant for determination of accurate defect concentrations at high temperatures.

4. Conclusion

It has been found that the obtained GaS monocrystals (hexagonal structure of sp.gr. $P6_3/mmc$: $a = 3.583$ Å, $c = 15.475$ Å) have a high specific resistance and band gap $\Delta E_g = 2.5$ eV at 300 K. Frequency dependences of alternating current conductivity across the layers of the GaS monocrystal before and after electron irradiation with various doses show that GaS conductivity decreases as a result of irradiation. The decrease in electrical conductivity of irradiated GaS can be related to compensation of the initially existing electrically active impurity centers by deep energy levels of radiation defects. Thus, irradiation of the GaS monocrystal causes radiation defects and stimulates the annealing and migration of defects existing in the crystal.

DFT calculations of band and electron structure in defective GaS supercells with 36 and 48 atoms made it possible to determine the electron density type and agree the values of ΔE_g between the calculation and the experiment. It has been established that the estimated enthalpy of GaS phase formation ($-\Delta_f H_f^{\circ}(\text{GaS}) = 1.95$ eV (or -188.4 kJ/mol) using the DFT method matches the experimental result, according to which the hexagonal phase ((sp.gr.) $P6_3/mmc$) is stable at low temperatures. The DFT calculation has also made it possible to estimate the degree of influence of disordered neutral atom vacancies on the GaS properties. The energies of neutral vacancy formation in GaS, taking into account the chemical potentials of Ga and S, agree with the published data.

The energy of Ga vacancy formation ($E_f^{\text{VxGa}} = 0.57$ eV) is lesser than that of S vacancies ($E_f^{\text{VxS}} = 0.62$ eV) in an oxidation atmosphere. The energy of S vacancy formation is lesser than that of Ga vacancies in a reducing atmosphere. From here it follows that the physical properties (electric,

optical etc.) greatly depend on the presence of defects in a layered GaS crystal. This also occurs due to disordering of Ga and S atoms across crystallographically non-equivalent sites of the GaS hexagonal structure. The obtained results can be used to make 2D-materials based on GaS with reproducible properties.

Acknowledgements

The work has been carried out with partial support from the Science Development Foundation with the President of the Republic of Azerbaijan (EIF) (grant No. EIF-BGM-3-BRFTF-2+/2017-15/05/1-M-13 and No. EIF-BGM-4-RFTF-1/2017-21/05/1-M-07) and the Russian Foundation for Basic Research (RFBR) (project No. Az_a2018).

Conflict of interest

The authors declare that they have no conflict of interest.

References

- [1] S.M. Asadov, S.N. Mustafayeva, V.F. Lukichev. *Russ. Microelectron.* **48**, 422 (2019). <https://doi.org/10.1134/S1063739719660016>
- [2] S.N. Mustafayeva, M.M. Asadov, A.A. Ismailov. *Phys. Solid State* **50**, 2040 (2008). <https://doi.org/10.1134/S1063783408110073>
- [3] N.Kh. Abrikosov, V.F. Bankina, L.V. Poretskaya, E.V. Skudnova, S.N. Chizhevskaya. *Poluprovodnikovye khalkogenidy I splavy na ikh osnove*. Nauka, M. (1975). 220 p. (in Russian).
- [4] *Semiconductors Data Handbook* / Ed. O. Madelung. Springer, Berlin (2004). <https://doi.org/10.1007/978-3-642-18865-7>
- [5] S.N. Mustafayeva, M.M. Asadov. *Solid State Commun.* **45**, 491 (1983). [https://doi.org/10.1016/0038-1098\(83\)90159-X](https://doi.org/10.1016/0038-1098(83)90159-X)
- [6] D. Wickramaratne, F. Zahid, R.K. Lake. *J. Appl. Phys.* **118**, 7, 075101 (2015). doi:10.1063/1.4928559
- [7] A. Kuhn, A. Bourdon, J. Rigoult, A. Rimsky. *Phys. Rev. B* **25**, 4081 (1982). <https://doi.org/10.1103/PhysRevB.25.4081>
- [8] Z.A. Dzhakhgirli. *Phys. Solid State* **54**, 1092 (2012). <https://doi.org/10.1134/S106378341205008>
- [9] V.V. Karpov, A.V. Bandura, R.A. Evarestov. *Phys. Solid State* **62**, 1017 (2020). <https://doi.org/10.1134/s1063783420060116>
- [10] S.N. Mustafayeva, M.M. Asadov. *Mater. Chem. Phys.* **15**, 185 (1986). [https://doi.org/10.1016/0254-0584\(86\)90123-9](https://doi.org/10.1016/0254-0584(86)90123-9)
- [11] G. Micocci, A. Serra, A. Tepore. *J. Appl. Phys.* **82**, 2365 (1997). <https://doi.org/10.1063/1.366046>
- [12] S. Shigetomi, T. Ikar. *J. Appl. Phys.* **95**, 6480 (2004). <https://doi.org/10.1063/1.1715143>
- [13] Y.-K. Hsu, C.-S. Chang, W.-C. Huang. *J. Appl. Phys.* **96**, 1563 (2004). <https://doi.org/10.1063/1.1760238>
- [14] M.M. Asadov, S.N. Mustafayeva, S.S. Guseinova, V.F. Lukichev. *Phys. Solid State* **62**, 2224 (2020). <https://doi.org/10.1134/S1063783420110037>
- [15] *Inorganic Nanosheets and Nanosheet-Based Materials. Fundamentals and Applications of Two-Dimensional Systems* / Eds T. Nakato, J. Kawamata, S. Takagi. Springer, Jpn KK (2017). 542 p. ISBN 978-4-431-56494-2
- [16] Y. Ni, H. Wu, C. Huang, M. Mao, Z. Wang, X. Cheng. *J. Cryst. Growth.* **381**, 10 (2013). <https://doi.org/10.1016/j.jcrysgro.2013.06.030>
- [17] T. Wang, J. Li, Q. Zhao, Z. Yin, Y. Zhang, B. Chen, Y. Xie, W. Jie. *Materials* **11**, 186 (2018). <https://doi.org/10.3390/ma11020186>
- [18] S.M. Asadov, S.N. Mustafayeva, A.N. Mammadov. *J. Therm. Anal. Calorim.* **133**, 1135 (2018). <https://doi.org/10.1007/s10973-018-6967-7>
- [19] H.L. Zhuang, R.G. Hennig. *Chem. Mater.* **25**, 3232 (2013). <https://doi.org/10.1021/cm401661x>
- [20] Y. Ma, Y. Dai, M. Guo, L. Yu, B. Huang. *Phys. Chem. Chem. Phys.* **15**, 7098 (2013). <https://doi.org/10.1039/C3CP50233C>
- [21] V. Zólyomi, N.D. Drummond, V.I. Fal'ko. *Phys. Rev. B* **87**, 195403 (2013). <https://doi.org/10.1103/PhysRevB.87.195403>
- [22] C.S. Jung, F. Shojaei, K. Park, J.Y. Oh, H.S. Im, D.M. Jang, J. Park, H.S. Kang. *ACS Nano* **9**, 9585 (2015). <https://doi.org/10.1021/acsnano.5b04876>
- [23] E.G. Seebauer, M.C. Kratzer. *Charged Semiconductor Defects. Structure, Thermodynamics and Diffusion*. Springer-Verlag London (2009). 294 p. ISBN 978-1-84882-058-6.
- [24] A. Alkauskas, P. Deák, J. Neugebauer, A. Pasquarello, C.G. Van de Walle. *Advanced Calculations for Defects in Materials (Electronic Structure Methods)*. Wiley-VCH Verlag & Co. KGaA, Boschstr. Weinheim, Germany (2011). 384 p. ISBN: 978-3-527-41024-8.
- [25] R.A. Evarestov. *Theoretical Modeling of Inorganic Nanostructures*. 2nd ed. Springer. Nature. Switzerland AG. (2020). 857 p. ISBN 978-3-030-42993-5
- [26] H. Chen, Y. Li, L. Huang, J. Li. *RSC Adv.* **5**, 50883 (2015). <https://doi.org/10.1039/C5RA08329J>
- [27] J.P. Perdew, W. Yue. *Phys. Rev. B* **33**, 8800 (1986). <https://doi.org/10.1103/physrevb.33.8800>
- [28] J.P. Perdew, J.A. Chevary, S.H. Vosko, K.A. Jackson, M.R. Pederson, D.J. Singh, C. Fiolhais. *Phys. Rev. B* **46**, 6671 (1992). <https://doi.org/10.1103/physrevb.46.6671>
- [29] J.P. Perdew, K. Burke, M. Ernzerhof. *Phys. Rev. Lett.* **77**, 3865 (1996). <https://doi.org/10.1103/physrevlett.77.3865>
- [30] M.M. Asadov, S.N. Mustafayeva, S.S. Guseinova, V.F. Lukichev, D.B. Tagiev. *Phys. Solid State* **63**, 797 (2021). <https://doi.org/10.1134/S1063783421050036>
- [31] H.J. Monkhorst. *Phys. Rev. B* **13**, 5188 (1976). <http://dx.doi.org/10.1103/PhysRevB.13.5188>
- [32] W.H. Press, S.A. Teukolsky, W.T. Vetterling, B.P. Flannery. *Numerical Recipes*. 3rd ed. Cambridge University Press, Cambridge (2007). 490 p. ISBN-13 978-0-511-33555-6
- [33] P. Perdew, W. Yang, K. Burke, Z. Yang, E.K.U. Gross, M. Scheffler, G.E. Scuseria, T.M. Henderson, I.Y. Zhang, A. Ruzsinszky, H. Peng, J. Sun, E. Trushin, A. Görling. *Proc. Nat. Acad. Sci.* **114**, 2801 (2017). <https://doi.org/10.1073/pnas.1621352114>
- [34] I. Barin, O. Knacke, O. Kubaschewski. *Thermochemical properties of inorganic substances*. Supplement, Springer-Verlag, Berlin. Heidelberg GmbH (1977). P. 270. ISBN 978-3-662-02295-5

- [35] O. Kubashewski, C.B. Alcock, P.J. Spencer. *Mater. Thermochem.* Pergamon. 6th ed. Press, Oxford, N.Y. (1993). 363 p. ISBN-13: 978-0080418896
- [36] A.S. Abbasov. *Termodinamicheskiye svoistva nekotorykh poluprovodnikovyykh veshchestv.* Izd-vo Elm., Baku (1981). 88 p. (in Russian).
- [37] C.G. Van de Walle, A. Janotti. *Advances in Electronic Structure Methods for Defects and Impurities in Solids / Eds A. Alkauskas, P. Deák, J. Neugebauer, A. Pasquarello, C.G. Van de Walle. Advanced Calculations for Defects in Materials (Electronic Structure Methods).* Wiley-VCH Verlag & Co. KGaA, Weinheim, Germany (2011). P. 1-16. ISBN:978-3-527-41024-8.
- [38] G. Job, R. Rüffler. *Physikalische Chemie.* Vieweg + Teubner Verlag. Springer Fachmedien Wiesbaden GmbH. (2011). ISBN 978-3-8351-0040